RESEARCH ARTICLE

Electrochemical and quantum chemical study to assess the role of (2E)-2-(furan-2-ylmethylidene) hydrazine carbothioamide as inhibitor for acid corrosion of mild steel

V. R. Adinarayanan[1] · P. Preethi Kumari[1] · Suma A. Rao[1]

Abstract

Synthesis and inhibition effectiveness of (2E)-2-(furan-2-ylmethylidene) hydrazine carbothioamide (FMHC) as an inhibitor for corrosion of mild steel in 0.5 M H_2SO_4 is reported. Experiments were conducted at various temperatures (303–323 K) by adopting potentiodynamic polarization and electrochemical impedance spectroscopy. Readings obtained demonstrated that percentage inhibition efficiency (% IE) improved with the upsurge in the concentration of FMHC, while it decreased with a rise in temperature. The highest % IE observed was 60% for 2.5×10^{-4} M FMHC at 303 K. FMHC worked moderately as a mixed inhibitor. FMHC obeyed the Langmuir model of adsorption and the mode of adsorption was physisorption on the mild steel surface which was further endorsed by examining the surface using the scanning electron microscope. A clear insight into the mechanistic features of corrosion inhibition by using FMHC was acquired. Calculation of activation parameters helped to suggest an appropriate mechanism for the adsorption of FMHC on mild steel through quantum chemical calculations using density functional theory (DFT).

Graphical abstract
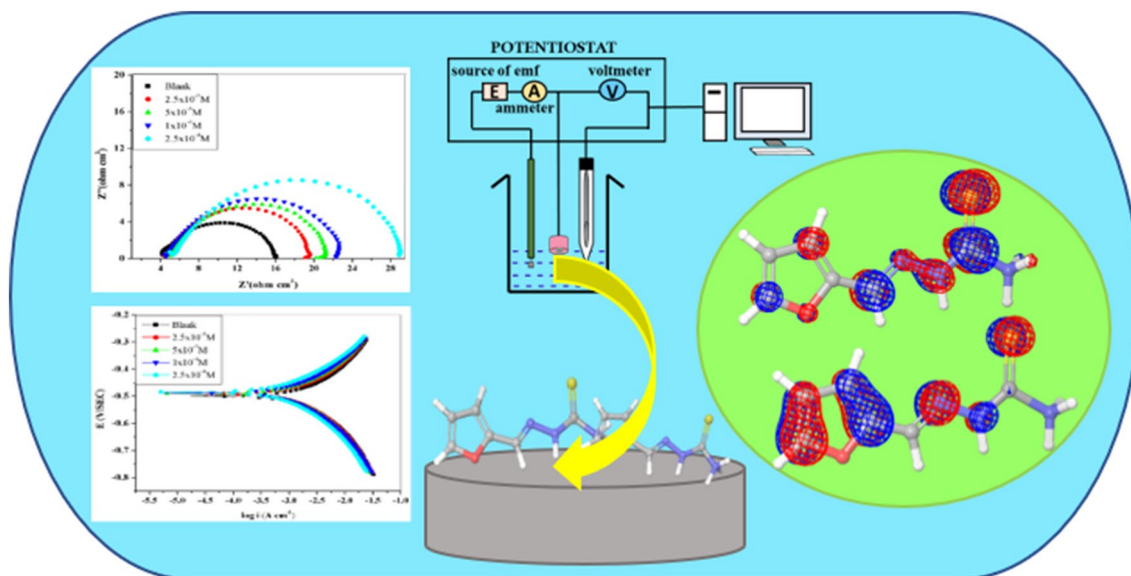
Keywords Mild steel · Hydrazine carbothioamide · Physisorption · Adsorption · Surface morphology · Density functional theory

---

Extended author information available on the last page of the article

1 Introduction

Mild steel due to its outstanding mechanical properties such as high tensile strength, impact strength, easy availability, low price is used in diverse industries such as construction or structural material, in chemical reactors, oil, and gas transport pipelines, manufacturing of automobiles, etc. [1]. The most commonly used acid solutions for removal of rust, de-scaling, and pickling before plating are hydrochloric acid and sulphuric acid [2]. Mild steel undergoes corrosion when exposed to acidic environments and hence their surface must be protected. Protection of metals from corrosion is important as corrosion leads to a great loss of material, as well as economy. The consequence of corrosion is tremendous, and its inhibition has been profoundly examined. It has been tracked down that perhaps the best strategy for protecting materials against electrochemical degradation includes the addition of inhibitors that are substances that minimize the rate of corrosion [3]. Subsequently, in the field of corrosion and industry, there is always a need to develop and use corrosion inhibitors which are an effective and reasonably low-cost method, to minimize the corrosive damage on materials. Literature reports indicated that usually compounds comprising of heteroatoms, unsaturated bonds, and aromatic or heterocyclic rings performed as inhibitors [4, 5]. Adsorption of inhibitor molecules on a material surface is responsible for corrosion inhibition. The adsorption relies fundamentally upon the electronic structure of the molecule. The effectiveness of the inhibitor relies upon its structure and the type of interaction with the metal surface [6].

To alleviate corrosion of mild steel in acid medium, hydrazide derivatives [7–11], thiosemicarbazide derivatives, acid hydrazide derivatives, and hydrazone derivatives [12–15] are reported. This is because of their exceptional structural features. The planarity of the whole structure of the compound dictates the formation of an adsorption film on the metal. [16]. As a part of our work on corrosion inhibition, we hereby report the corrosion rates of mild steel in 0.5 M H_2SO_4, determined by electrochemical techniques and its inhibition by (2E)-2-[Furan-2-ylmethylidene] hydrazine

carbothioamide (FMHC) at three different temperatures. The synthesized inhibitor possesses a linear structure with active centers like heteroatoms, electron-donating groups, etc., which is the major requirement of efficient inhibitor.

2 Experimental details

2.1 Material

The composition of the test coupon of mild steel utilized for corrosion study is given in Table 1.

2.2 Test specimen preparation

The mild steel test specimen was readied by means of cold setting resin. The uncovered level surface (1 cm^2) of the mounted part was subjected to polishing with different coarseness levels of emery papers and later the surface was finished by disc polishing with levigated alumina. Test coupon was washed with water, acetone and dried.

2.3 Preparation of medium

The stock of 1 M solution of H_2SO_4 was prepared from AR H_2SO_4. The solution was standardized by volumetric titration. As and when required from the stock, by proper dilution, the desired concentration was prepared.

2.4 Synthesis of (2E)-2-(furan-2-ylmethylidene) hydrazine carbothioamide (FMHC)

As per the reported literature, [17] (2E)-2-(furan-2-ylmethylidene) hydrazine carbothioamide (FMHC) was synthesized. An equimolar mixture of furan-2-aldehyde and thiosemicarbazide with sulphuric acid was refluxed on a boiling water bath for around 4 h. Ethanol was used for the recrystallization of the precipitated product. The scheme for the preparation of FMHC is given in Fig. 1. The characterization was done by IR and spectra is shown in Fig. 2.

Table 1 Composition of specimen

Element	C	Si	Mn	P	S	Cr	Ni	Mo	Al	Cu	Fe
(%wt.),	0.169	0.188	0.414	0.060	0.042	0.020	0.028	0.018	0.004	0.072	Balance

Fig. 1 Synthetic route for FMHC

furan-2-aldehyde   Thiosemicarbazide   (2E)-2-(furan-2-ylmethylidene)hydrazinecarbothioamide
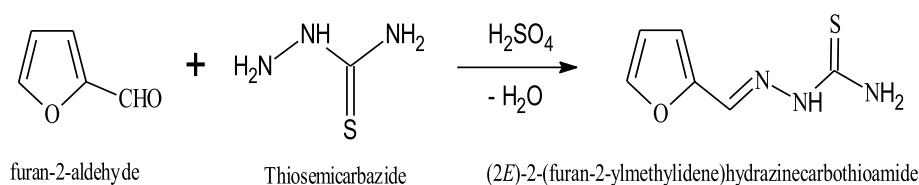
Fig. 2 IR spectra of FMHC. C$_6$H$_7$N$_3$OS m. p: 230—232 °C IR (KBr) [cm^{-1}]: 3255.95 (OH *str.*), 3186 (NH *str.*), 3035 (Ar. CH *str.*), 1614(C=O), 1600 (C=N *str.*), and 1600 (Ar. C=C *str.*)
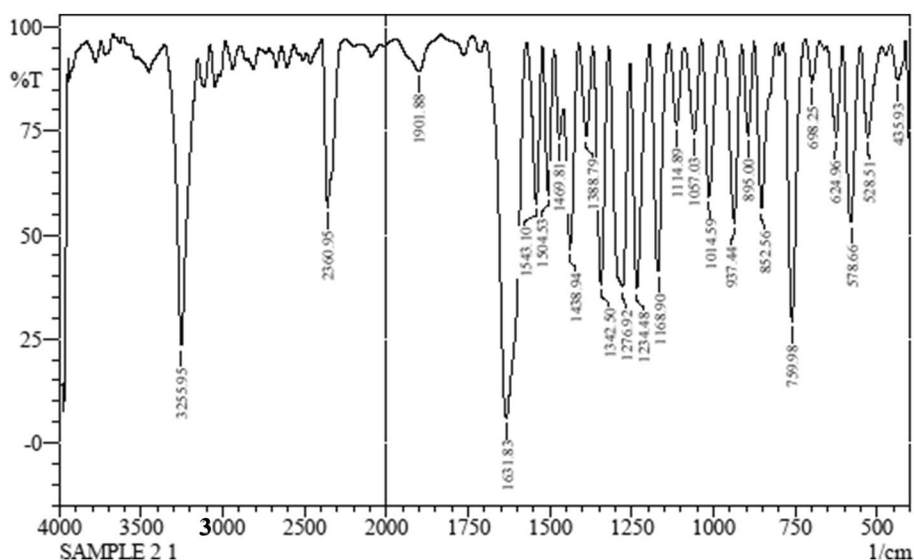
2.5 Electrochemical studies

Electrochemical examinations were performed with a potentiostat (USA Model 604D with beta programming). Pyrex glass cell with 3 electrodes, namely, counter (platinum), saturated calomel reference electrode (SCE), and the working electrode (mild steel) was used. A finely polished mild steel test coupon was introduced to 0.5 M sulphuric acid in the absence and presence of the inhibitor at various temperatures (303–323 K) and endorsed to establish an open circuit potential (OCP). PDP plots were recorded by drifting the potential of the test specimen to −250 mV cathodically and +250 mV anodically with respect to the OCP for a sweep speed of 0.5 mV s^{-1} [18]. The impedance tests were done by applying in the periodic AC signal of 10 mV in the wide frequency range of 100 kHz to 0.01 Hz on the OCP [19].

2.6 Surface studies

Scanning electron microscopy (SEM) images of test specimen were noted using (JEOL JSM-6380 L) scanning electron microscope. The surface of the corroded sample was studied by dipping it in 0.5 M sulphuric acid solution for 3 h in absence and presence of FMHC.

2.7 Quantum chemical calculations

Schrodinger programming (Maestro Material Science) was utilized to do quantum chemical estimations. The DFT was used to optimize the geometry of inhibitor FMHC. Computations were done using the Hybrid functional with the correlation functional (B3LYP) and 6-31G** as the basis set. For neutral and protonated FMHC, frontier molecular orbital (FMO) energies were determined and explained in depth.

Distinctive hypothetical parameters like the energy gap(ΔE), hardness (η), softness(σ), electronegativity (χ), electrophilicity (ω), nucleophilicity (ε), and portion of electron transferred (ΔN) were assessed utilizing appropriate equations [20–22]. Mulliken charge population was assessed. The dipole moment of protonated and neutral FMHC was found and compared.

3 Results and discussion

3.1 Potentiodynamic polarization studies

The potentiodynamic polarization graphs for mild steel in 0.5 M H$_2$SO$_4$ at 313 K without and with the addition of FMHC are shown in Fig. 3. Electrochemical parameters such as corrosion potential (E_{corr}), corrosion current density (i_{corr}), cathodic slope ($-\beta_c$), and anodic slope (β_a) were noted and corrosion rate (CR) and percentage inhibition efficiency (%IE) were calculated [23] using Eqs. (1) and (2), respectively.

$$CR\left(mmy^{-1}\right) = \frac{3270 \times M \times i_{corr}}{d \times n} \quad (1)$$

$$IE\% = \left(\frac{i_{corr} - i_{corr(inh)}}{i_{corr}}\right) \times 100 \quad (2)$$

i_{corr} and $i_{corr(inh)}$ are corrosion current density (μA cm^{-2}) in the absence and presence of the inhibitor, 3270 is a constant, M is the atomic mass of corroding material [55.85], d = density of corroding material (7.725 g cm^{-3}), and n is the
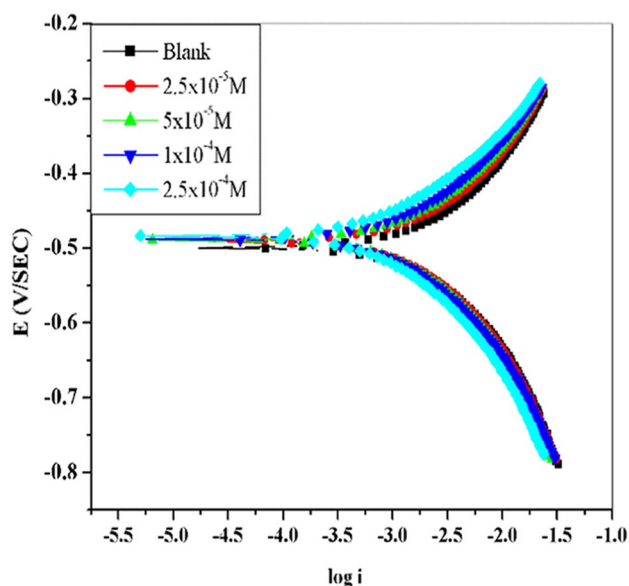
Fig. 3 PDP plot for corrosion of mild steel in presence of diverse FMHC concentrations in 0.5 M H$_2$SO$_4$ at 313 K

number of electrons involved in the reaction ($n=2$). Fraction of surface covered (θ) is calculated using Eq. (3)

$$\%IE = \theta \times 100 \tag{3}$$

From Fig. 3, it was seen that the corrosion potential does not shift much with respect to blank. The slight difference in the cathodic and anodic slope shows the influence of the inhibitor FMHC on the reaction kinetics but not on the mechanism [24, 25]. The results of Tafel polarization are tabulated in Table 2.

From Table 2 it is evident that the corrosion rate of mild steel amplified with the upsurge in temperature in absence of FMHC. Added FMHC lessened the rate of corrosion. IE decreased with an increase in temperature. The exothermic nature of the adsorption process is suggestive of physical adsorption [26].

3.2 Electrochemical impedance spectroscopy

The Nyquist plot for the corrosion of mild steel in 0.5 M H$_2$SO$_4$ is shown in Fig. 4. The plot consists of two loops. One loop is high-frequency (HF) capacitive loop and another is small inductive loop at medium frequency (MF). Capacitive loop at high frequency stands for resistance for charge transfer. Diameter of the capacitive loop increased after the addition of inhibitor and increased further with increase in concentration of inhibitor. It clearly demonstrated the ability of inhibitor molecule to bring down the rate of charge transfer and hence corrosion [27]. Small inductive loop could be due to relaxation effect either due to hydrogen ion or corrosion product or metal ion inhibitor complex.

The appropriate equivalent circuit was used to simulate the impedance data with FMHC as shown in Fig. 4b. It consisted of 5 elements. They are solution resistance (R_s), charge transfer resistance (R_{ct}), time constant phase element (Q), an inductive element (L), and inductive resistance (R_L) [28].

The collective resistance due to the charge transfer and inductive loop is considered polarization resistance (R_p). It is calculated as per Eq. (4)

Table 2 Results of PDP measurements

| Temp (K)	FMHC$\times 10^{-5}$ (M)	E_{corr} (mV)	$-\beta_c$ (mVdec^{-1})	β_a (mVdec^{-1})	CR (mmy^{-1})	i_{corr} (mA cm^{-2})	IE (%)
303	0.0	−499	71.69	71.32	7.437	1.259	0
	2.5	−492	66.37	72.70	6.017	1.018	19.14
	5.0	−490	72.27	77.11	4.932	0.834	33.68
	10.0	−486	74.38	81.42	4.630	0.783	37.73
	25.0	−481	75.39	88.91	2.946	0.448	60.00
313	0.0	−497	68.04	66.08	10.871	1.840	0
	2.5	−491	73.24	70.62	8.133	1.518	17.50
	5.0	−490	75.09	74.16	7.366	1.247	32.22
	10.0	−486	78.16	75.50	6.911	1.170	36.41
	25.0	−480	77.09	82.61	4.505	0.762	58.00
323	0.0	−497	63.88	61.78	14.216	2.406	0
	2.5	−491	56.97	63.65	13.423	2.105	12.48
	5.0	−488	63.17	68.03	12.440	1.675	30.38
	10.0	−492	67.33	71.18	9.362	1.585	34.12
	25.0	−480	67.39	76.83	8.453	1.328	44.80
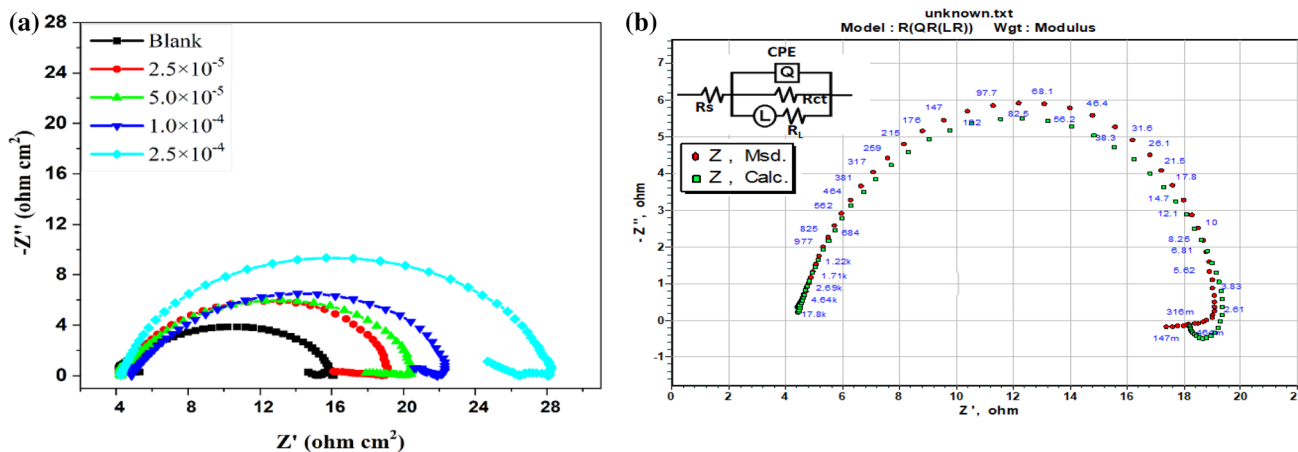
Fig. 4 **a** Nyquist plots **and b** equivalent circuit fitment

$$R_p = \frac{R_{ct} \times R_L}{R_{ct} + R_L} \tag{4}$$

The increase in the concentration of inhibitor added tends to decrease the double-layer capacitance (C_{dl}) because of the decrease in the double-layer thickness [29]. CPE acts as an ideal double-layer capacitance (C_{dl}). It was calculated from the frequency (f_{max}) at which the imaginary component of impedance becomes maximum (Zimp, max) using Eq. (5)

$$C_{dl} = \frac{1}{2\pi R_{ct}f_{max}} \tag{5}$$

Calculation of percentage inhibition was done using Eq. (6)

$$IE(\%) = \frac{R_{ct(inh)} - R_{ct}^0}{R_{ct(inh)}} \tag{6}$$

where R_{ct} and R_{ct}^0 show the charge transfer resistance in the presence and absence of inhibitor. Results are tabularized in Table 3

It is evident from Table 3 that the C_{dl} values decreased with a rise in inhibitor concentration at all studied temperatures. Increased R_{ct} values at increased concentrations of FMHC resulted in improved corrosion resistance. This suggests the presence of a barrier layer on the electrode surface. The results obtained by the PDP and EIS method for the corrosion of mild steel in 0.5 M H_2SO_4 with FMHC were in good agreement at all studied temperatures.

3.3 Effect of temperature

Influence of temperature on the corrosion rate of mild steel and inhibition efficiency of inhibitor was studied at temperatures range of 303 K to 323 K. Figure 5 depicts the

variation of % *IE* at varying concentrations of FMHC at different temperatures.

Using Arrhenius equation (Eq. 7), calculation of the activation energy (E_a) was done

$$\ln(CR) = B - \frac{E_a}{RT} \tag{7}$$

where B = Arrhenius pre-exponential constant and R = universal gas constant.

The slope of the plot of ln CR vs 1/T (Fig. 6a) [30] is used to calculate the activation energy. Enthalpy of activation (ΔH_a) and entropy of activation (ΔS_a) were found out using the transition state Eq. (8)

$$CR = \frac{RT}{Nh} \exp\left(\frac{\Delta S^\#}{RT}\right) \exp\left(\frac{-\Delta H^\#}{RT}\right) \tag{8}$$

Here h is Planck's constant and N is Avogadro's number. Plot of ln(CR/T) vs 1/T [Fig. 6b] gave a straight line. From slope and intercept, activation parameters were evaluated and recorded in Table 4.

The increase in activation energy indicates an increase in the energy barrier for the corrosion reaction. E_a values increased with an increase in FMHC concentration suggesting the physisorption. The negative value of entropy of activation (ΔS_a) indicates the association process during the formation of the activated complex [31, 32].

3.4 Adsorption isotherm

Adsorption isotherm provides evidence for interaction among inhibitor and metal surface. It enables the understanding of the mechanism of corrosion inhibition. FMHC adsorbs on the metal surface and forms a barricade over it and isolates the metal surface from the medium. The efficiency of the inhibitor

Table 3 Results of EIS measurements

Temp. (K)	FMHC×10^{-5} (M)	R_{ct} (Ω cm^{-2})	R_L (Ω cm^{-2})	R_p (Ω cm^{-2})	C_{dl} (μF cm^2)	IE (%)
303	0.0	16.74	118.9	14.67	1033.7	–
	2.5	20.11	162.1	17.89	679.43	18.00
	5.0	22.50	219.4	20.41	440.84	28.11
	10.0	27.20	251.8	24.55	285.76	40.24
	25.0	50.20	295.0	42.90	123.32	65.80
313	0.0	12.13	84.63	10.61	3032.1	–
	2.5	14.37	114.4	12.77	2362.3	16.90
	5.0	16.54	115.9	14.47	1842.7	26.70
	10.0	19.01	120.2	16.41	1481.0	35.36
	25.0	23.75	268.7	21.82	774.66	51.38
323	0.0	10.15	67.57	8.82	4748.6	–
	2.5	11.35	75.20	9.86	3588.2	10.52
	5.0	13.51	98.65	11.88	2617.3	25.74
	10.0	15.02	105.2	13.14	2096.1	32.86
	25.0	18.26	145.6	16.23	1603.6	45.61
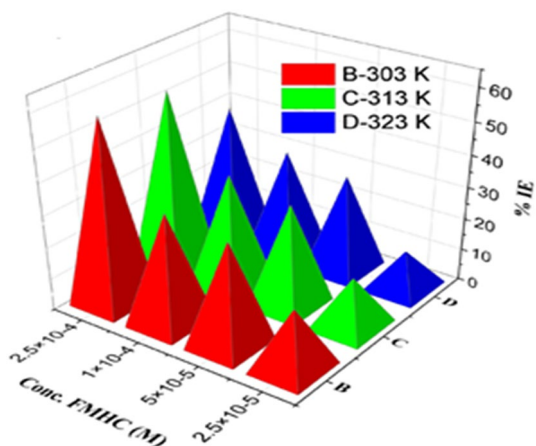
Fig. 5 Variation of % *IE* with temperatures and FMHC concentrations

depends on the degree of surface coverage (θ). Linear fit of parameters to several adsorption isotherms in the temperature range was considered, and Langmuir's adsorption isotherm was obeyed. It is given by the expression (9)

Table 4 Activation parameters

FMHC×10^{-5} (M)	E_a (kJ mol^{-1})	ΔH_a (kJ mol^{-1})	$-\Delta S_a$ (J K^{-1} mol^{-1})
0	26.39	23.79	149.61
2.5	32.54	29.94	131.50
5.0	37.57	34.97	116.48
10.0	28.67	26.07	146.05
25.0	42.77	40.17	103.70
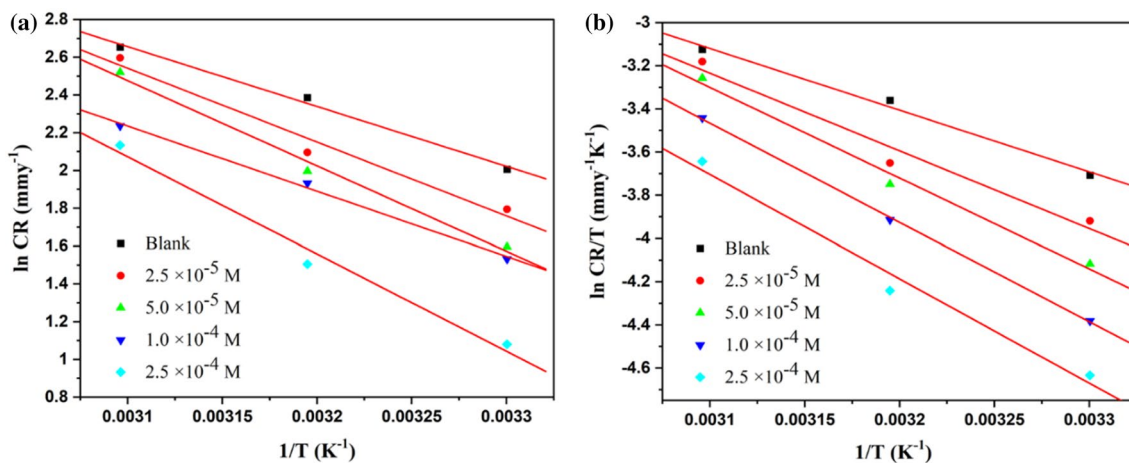
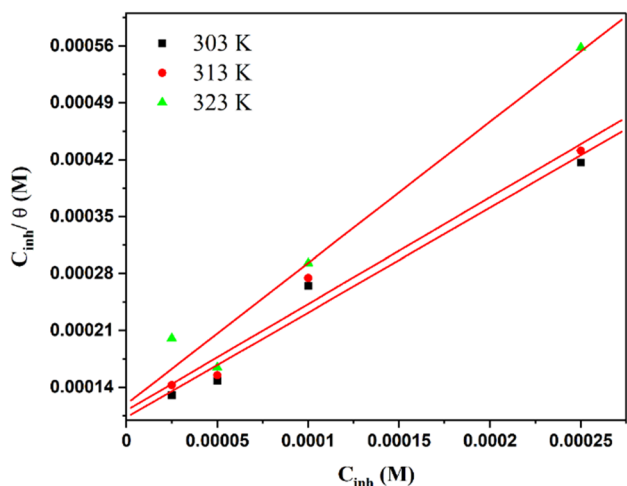**Fig. 6** Plot of **a** ln(CR) Vs (1/*T*) and **b** ln(CR/T) vs 1/*T*

Fig. 7 Langmuir adsorption isotherm

$$\frac{C_{inh}}{\theta} = \frac{1}{K} + C_{inh} \qquad (9)$$

where the K value indicates the equilibrium constant for metal-inhibitor interaction, C_{inh} is the inhibitor concentration, and θ is the degree of surface coverage [33]. The plots of C_{inh}/θ versus C_{inh} for different temperatures give a straight line with intercept $1/K$ as shown in Fig. 7.

Standard free energy of adsorption $\left(\Delta G^0_{ads}\right)$ is related to adsorption/desorption constant (K) by relation (10)

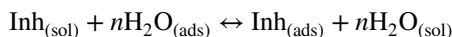$$K = \frac{1}{55.5} \exp\left(\frac{-\Delta G^0_{ads}}{RT}\right) \qquad (10)$$

where R is the universal gas constant, T is absolute temperature, and 55.5 is the concentration of water in solution in mol dm^{-3} [34].

As per the reported literature [35, 36] ΔG^0_{ads} more negative than -40 kJ mol^{-1} is suggestive of chemical adsorption. However, in the present study value of ΔG^0_{ads} is found to be between -33 kJ mol^{-1} and -35 kJ mol^{-1}. It is clearly suggestive of physical adsorption. In order to get a clear-cut picture of the

nature of adsorption, detailed quantum chemical calculations are done and discussed in Sect. 3.6

3.5 Role of FMHC in corrosion inhibition

Adsorption of FMHC is a consequence of the replacement of water molecules which is usually adsorbed on the metal surface.

$$Inh_{(sol)} + nH_2O_{(ads)} \leftrightarrow Inh_{(ads)} + nH_2O_{(sol)}$$

$$6H_2SO_4 + 3Fe \rightarrow 3Fe(HSO_4)_2 + 3H_2$$

$$3Fe(HSO_4)_2 \rightarrow Fe_3(SO_4)_2 + 4H_2SO_4$$
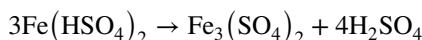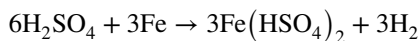
The metal surface is positively charged when in contact with H_2SO_4 [37]. Because of the accumulation of positive charges at the interface, sulfate ions get adsorbed here because of electrostatic interaction, leading to the formation of the electrical double layer. These negative charges will allure protonated FMHC for adsorption. In this way, protonated FMHC gets electrostatically adsorbed on mild steel, which was previously covered with sulfate ions. Likewise, at cathodic regions also, protonated FMHC gets adsorbed thereby decreasing the rate of hydrogen evolution [38, 39]. Schematic illustration of corrosion inhibition mechanism of FMHC is depicted in Fig. 8.

3.6 Quantum chemical study

As per Pearson's Hard Soft Acid–Base (HSAB) theory, the energy gap is difference between the highest occupied molecular orbital (E_{HOMO}) and lowest unoccupied molecular orbital (E_{LUMO}) of the inhibitor molecule [40]. Further, E_{HOMO} is directly connected to ionization energy and E_{LUMO} is directly linked to electron affinity. Hence liability of a molecule toward electrophilic attack is designated by E_{HOMO}, while the vulnerability of a molecule toward nucleophilic attack is shown by E_{LUMO} [41]. Optimized

Fig. 8 Schematic representation of the mechanism of corrosion inhibition by FMHC
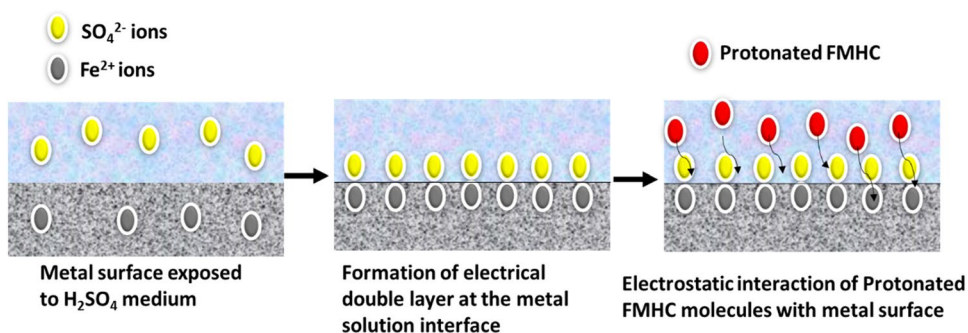
structures of FMHC and frontier orbital electron density distribution for neutral FMHC are shown in Fig. 9.

FMHC gets protonated in an aqueous acidic medium and involves in the physical adsorption process. Optimized structure and frontier orbital electron density distribution for protonated FMHC are shown in Fig. 10.

It becomes essential to know the electron population or electron density distribution within the inhibitor molecule. The preferred site for protonation of FMHC is heteroatom with remarkably high negative Mulliken charges. [42, 43]. Mulliken charge distribution in various heteroatoms present in FMHC is given in Fig. 11 and Table 5.

Table 6 reports the various parameters of the quantum chemical study of FMHC (for neutral and protonated molecules) [44–47].

When E_{HOMO} of the neutral molecule is associated with that of protonated FMHC, there is a diminution in the value showing that electron-donating ability decreased significantly after protonation. Further, the E_{LUMO} value also reduced to a significant extent suggesting that the electron-accepting capacity of the FMHC increased. After protonation, the global electronegativity (χ) increased twofold. Electrophilicity index (ω) increased, and nucleophilicity (ϵ) decreased to a large extent in the case of protonated FMHC. This led to stable layer formation on the surface of mild steel as a decrease in the energy gap (ΔE,) between E_{HOMO} and E_{LUMO}. For a neutral FMHC, the fraction of electron transferred (ΔN) is 0. 26, whereas for protonated FMHC molecule, it is − 1.63. This suggested that a neutral molecule can give electrons, whereas after protonation, its electron giving capacity is reduced and its tendency to

**Fig. 9** Optimized structure and frontier orbital electron density distribution for neutral FMHC

NEUTRAL OPTIMIZED STRUCTURE   NEUTRAL HOMO

ΔE= 3.7452

NEUTRAL LUMO
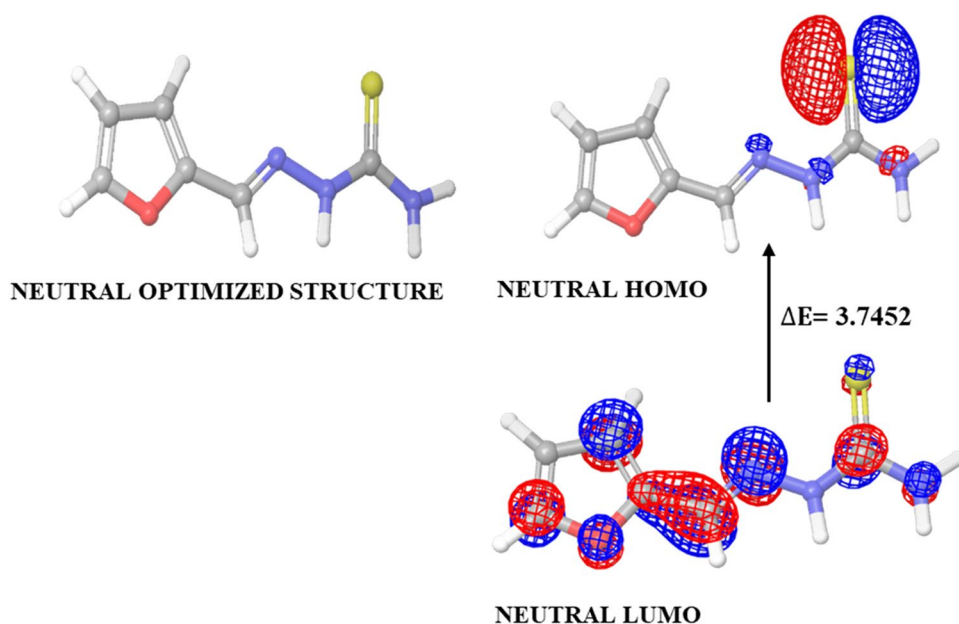
Fig. 10 Optimized structure of protonated inhibitor molecule and its frontier electron density distribution

PROTONATED OPTIMIZED STRUCTURE   PROTONATED HOMO

ΔE= 3.3306
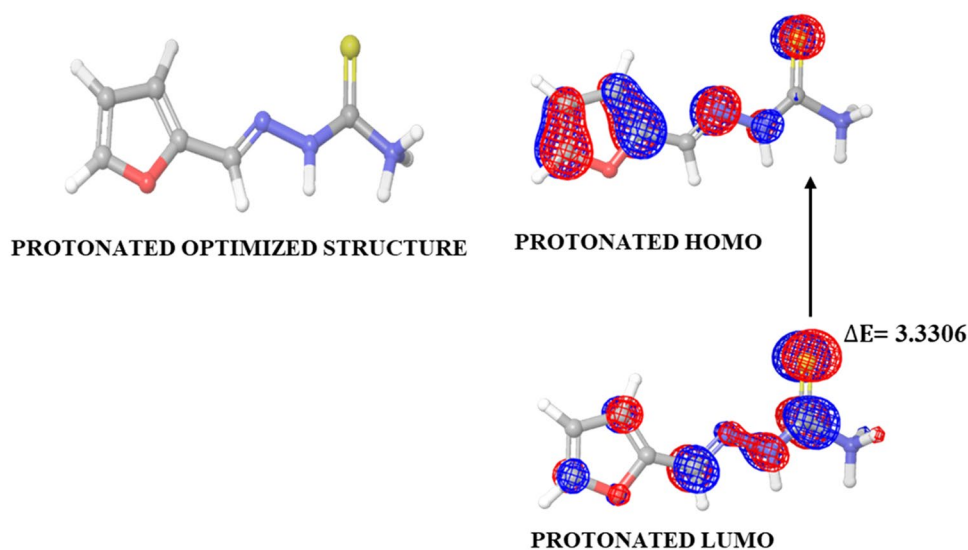
PROTONATED LUMO

Fig. 11 Mulliken charge distribution
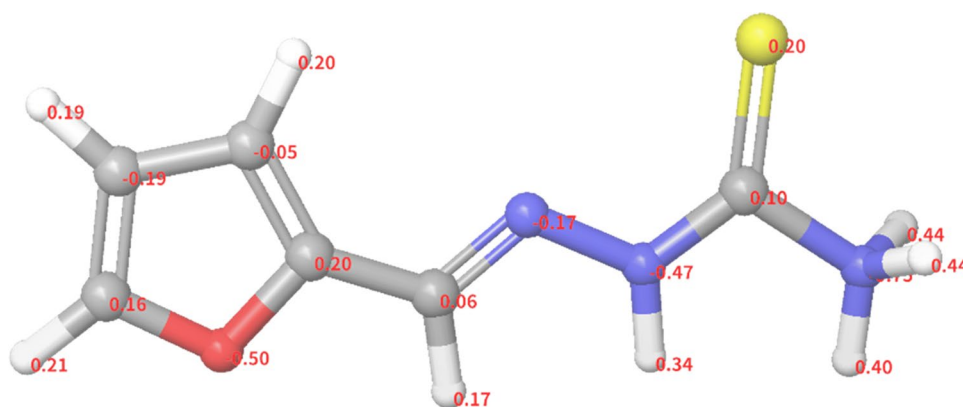
Table 5 Mulliken charges on heteroatoms of FMHC

Mulliken charge	O(1)	N(7)	N(8)	N(10)	S(7)
Neutral	− 0.521	− 0.131	− 0.521	− 0.721	− 0.08
Protonated	− 0.500	− 0.166	− 0.469	− 0.745	0.19

receive electrons increased many folds [44]. This again reaffirmed the physisorption of protonated FMHC molecules onto the surface of mild steel.

The dipole moment (μ) of the neutral FMHC is 1.150 Debye. After protonation, the dipole moment is 8.811 Debye. The large increase in the value of dipole moment for protonated molecule compared to that of water molecule confirmed its physical adsorption on metallic surface replacing water molecule [48].

3.7 Surface morphology studies

The impact of FMHC on corrosion of mild steel was evaluated by recording the SEM pictures. Mild steel was immersed in 0.5 M H_2SO_4 for 3 h with and without inhibitor. Figure 12a

shows the pits because of the destructive activity of 0.5 M H_2SO_4 on the mild steel surface with cracks and unpleasant, uneven, in homogeneous surface. Figure 12b depicts steel surface after immersion in 0.5 M H_2SO_4 containing 2.5×10^{-4} M FMHC. It is quite evident that surface has become relatively smooth in large area due to the adsorption of FMHC.

4 Conclusions

1. The effectiveness of FMHC increased with its concentration and lessened at elevated temperatures.
2. FMHC performed as a moderate mixed type of inhibitor, endured physical adsorption, and adapted Langmuir's adsorption isotherm.
3. FMHC showed inhibition efficiency of 60% at concentration of 2.5×10^{-4} M at 303 K.
4. Surface studies confirmed the adsorption of FMHC on the metal.
5. Quantum chemical calculations supported the mechanistic aspect of corrosion.

Table 6 Quantum chemical parameters of the neutral and protonated FMHC

	E_{HOMO}	E_{LUMO}	ΔE	χ	η	σ	ω	ε	ΔN	μ
Neutral	− 5.3850	− 1.6398	3.7452	3.5124	1.8726	0.5340	1.6470	0.6071	0.26	1.150
Protonated	− 9.4449	− 6.1143	3.3306	7.7796	1.6653	0.6004	9.0857	0.110	− 1.63	8.811

Units: Energy—eV; μ—Debye; σ—eV^{-1}
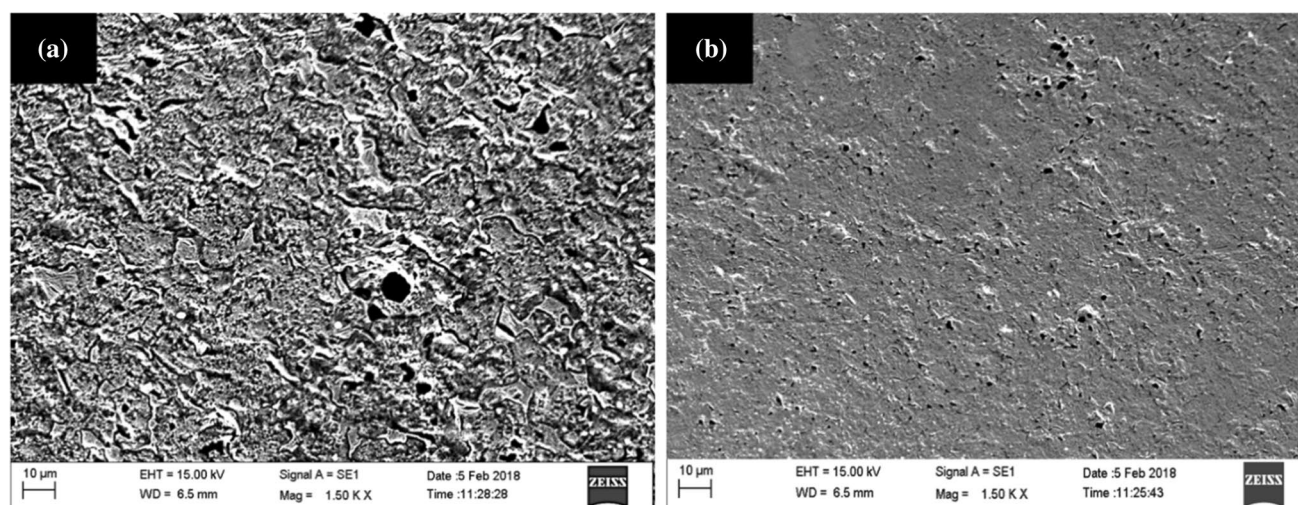
Fig. 12 SEM images: **a** MS + 0.5 M H$_2$SO$_4$ **and b** MS + 0.5 M H$_2$SO$_4$ + 2.5 × 10^{-4} M of FMHC

Declarations

Conflict of interest On behalf of all authors, the corresponding author claims no conflict of interest.

References

1. Prabhu RA, Venkatesha TV, Shanbhag AV, Praveen BM et al (2008) Quinol-2-thione compounds as corrosion inhibitors for mild steel in acid solution. Mater Chem Phys 108:283–289. https://doi.org/10.1016/j.matchemphys.2007.09.038
2. Narayan R (1993) An introduction to metallic corrosion and its prevention. Oxford and IBH Publishing Co, New Delhi
3. Sathiyanarayanan AS, Jeyaprabha C, Muralidharan S, Venkatachari G (2006) Inhibitionof iron corrosion in 0.5 Msulphuric acid by metal cations. Appl Surf Sci 252:8107–8112. https://doi.org/10.1016/j.apsusc.2005.10.028
4. Mercer AD (1994) Corrosion inhibition: principles and practice. In: Shreir LL, Jarman RA, Burstein GT (eds) Corrosion control. Butterworth Heinemann, Oxford
5. Revie W, Uhlig's (2000) Corrosion handbook, 2nd edn. Wiley, NewYork
6. Kumari P, Shetty P, Rao SA, Sunil D (2014) Corrosion inhibition and adsorption behaviour of (2E)-2-(3-hydroxy benzylidene) hydrazine carbothiamide on mild steel in 1M HCl. Rev Roum Chim 59(5):323–333
7. Saliyan R, Adhikari V (2008) Quinolin-5-ylmethylene-3-{[8-(trifluoromethyl)quinolin-4- yl]thio}propanohydrazide as an effective inhibitor of mild steel corrosion in HCl solution. Corros Sci 50:55–61. https://doi.org/10.1016/j.corsci.2006.06.035
8. Mohan P, Arunsunai KK, Paruthimal KG, Muralidharan VS (2012) N′- (4-Methoxy benzylidene)benzo hydrazideas effective corrosion inhibitor for mild steel in 1 M HCl. Asian J Chem 24:5821–5823
9. Fouda AS, Mohamed MT, Soltan MR (2013) Role of some benzo hydrazide derivatives as corrosion inhibitorsfor carbon steel in HCl solution. J Electrochem Sci Technol 4:61–70. https://doi.org/10.5229/JECST.2013.4.2.61
10. Yadav M, Sinha RR, Kumar S, Bahadur I, Ebenso EE (2015) Synthesis and application of new acetohydrazide derivatives as a corrosion inhibition of mild steel in acidic medium: insight from electrochemical and theoretical studies. J Mol Liq 208:322–332. https://doi.org/10.1016/j.molliq.2015.05.005
11. Larabi L, Harek Y, Benali O, Ghalemb S (2005) Hydrazide derivatives as corrosion inhibitors for mild steel in 1M HC. Prog Org Coat 54:256–262. https://doi.org/10.1016/j.porgcoat.2005.06.015
12. Khaled KF, Elhabib OA, El-mghraby A, Ibrahim OB, MagdyIbrahim AM (2010) Inhibitive effect of thiosemicarbazone derivative on corrosion of mild steel in hydrochloric acid solution. J Mat Environ Sci 3:139–150
13. El-Shafei AA, Moussa MNH, El-FarAA (2001) The corrosion inhibition character of thiosemicarbazide and its derivatives for C-steel in hydrochloric acid solution. Mat Chem Phys 70:175–180. https://doi.org/10.1016/s0254-0584(00)00496-x
14. Saliyan R, Adhikari V (2009) Corrosion inhibition of mild steel in acid media by quinolinylthiopropanohydrazones. Indian J Chem Technol 16:162–174
15. Goulart CM, SouzaAE HCAM, Rodrigues CJF, Maciel MAM (2013) Experimental and theoretical evaluation of semicarbazones

and thiosemicarbazones as organic corrosion inhibitors. Corros Sci 67:281–291. https://doi.org/10.1016/j.corsci.2012.10.029

16. Emregül KC, Hayvalı M (2004) Studies on the effect of vanillin and protocatechualdehyde on the corrosion of steel in hydrochloric acid. Mater Chem Phys. https://doi.org/10.1016/j.matchemphys.2003.08.030

17. Renata BO, Elaine MSF, Rodrigo PPS, Anderson AA, Antoniana UKC (2008) Synthesis and antimalarial activity of semicarbazone and thiosemicarbazone derivatives. Eur J Med Chem 43:1983–1988. https://doi.org/10.1016/j.ejmech.2007.11.012

18. Uhlig HH, Revie RW (2008) Corrosion and corrosion control, 4th edn. Wiley, Hoboken

19. Prakashaiah BG, Vinaya Kumara D, Anup Pandith A, Nityananda Shetty A, Amitha Rani BE (2018) Corrosion inhibition of 2024–T3 aluminum alloy in 3.5% NaCl by thiosemicarbazone derivatives. Corros Sci 136:326–338. https://doi.org/10.1016/j.corsci.2018.03.021

20. Singh P, Ebenso EE, Olasunkanmi LO, Obot IB, Quraishi MA (2016) Electrochemical, theoretical, and surface morphological studies of corrosion inhibition effect of green naphthyridine derivatives on mild steel in hydrochloric acid. J Phys Chem C 120:3408–3419. https://doi.org/10.1021/acs.jpcc.5b11901

21. Verma C, Olasunkanmi LO, Ebenso EE, Quraishi MA, Obot IB (2016) Adsorption behavior of glucosamine-based, pyrimidine-fused heterocycles as green corrosion inhibitors for mild steel: experimental and theoretical studies. J Phys Chem C 120:11598–11611. https://doi.org/10.1021/acs.jpcc.6b04429

22. Ansari KR, Quraishi MA, Singh A, Ramkumar S, Obote IB (2016) Corrosion inhibition of N80 steel in 15% HCl by pyrazolone derivatives: electrochemical, surface and quantum chemical studies. RSC Adv 6:24130–24141. https://doi.org/10.1039/c5ra25441h

23. Yudhistira R, Kumari P, Sunil D, Shetty P, Rao SA (2019) Attenuation of acid corrosion of mild steel using a novel organic dye: electrochemical and surface measurements. Surf Eng Appl Electrochem 55:443–454

24. Khadiri A, Saddik R, Bekkouche K, Aouniti A, Hammouti B, Benchat N, Bouachrine M, Solmaz R (2016) Gravimetric, electrochemical and quantum chemical studies of some pyridazine derivatives as corrosion inhibitors for mild steel in 1 M HCl solution. J Taiwan Inst Chem Eng 58:552–564. https://doi.org/10.1016/j.jtice.2015.06.031

25. Abd El-Maksoud SA, Fouda AS (2005) Some pyridine derivatives as corrosion inhibitors for carbon steel in acidic medium. Mater Chem Phys 93:84–90. https://doi.org/10.1016/j.matchemphys.2005.02.020

26. Kumari P, Rao SA, Shetty P, Sunil D (2014) Corrosion inhibition and adsorption behavior of (2E)-2-(3-hydroxy-2-methoxybenzylidee hydrazine carbothioamide on mild steel in 0.5 HCl. Rev Roum Chem Phys 59(5):323–333

27. Li W, He Q, Jhang S (2008) Some new triazole derivatives as inhibitors for mild steel corrosion in acidic medium. J Appl Electrochem 38:289–290

28. Lagrenee M, Mernari B, Bouanis M, Traisnel M, Bentiss F (2002) Study of the mechanism and inhibiting efficiency of 3,5-bis(4-methylthiophenyl)-4H-1,2,4-triazole on mild steel corrosion in acidic media. Corros Sci 44(3):573–588. https://doi.org/10.1016/S0010-938X(01)00075-0

29. Kumari P, ShettyP RSA (2014) Corrosion inhibition effect of 4-hydroxy-N-[E-(1H-indole-2-ylmethylidene)] benzohydrazide. Int J Corros. https://doi.org/10.1155/2014/256424

30. Kumar P, Shetty AN (2013) Electrochemical investigation on the corrosion of 18%Ni M250 grade maraging steel under welded condition in sulfuric acid medium. Surf Eng Appl Electrochem 49:253–260

31. AnbarasiCM AuxiliaAJ (2016) Surface modification of carbon steel by hexanesulphonic acid-Ni^{2+} system and its corrosion study. Int J Chem Tech Res 9:218–225

32. Keles H, Keles M (2014) Electrochemical investigation of a Schiff base synthesized by cinnamaldehyde as corrosion inhibitor on mild steel in acidic medium. Res Chem Intermed 40:193–209

33. OguzieEE NVO, Enenebeaku CK, AkaleziCO OC (2008) Effect of hexamethylpararosaniline chloride (crystal violet) on mild steel corrosion in acidic media. Corros Sci 50:3480–3486

34. Migahed MA, MohammedHM A-S (2003) Corrosion inhibition of H-11 type carbon steel in 1 M hydrochloric acid solution by N-propyl amino lauryl amide and its ethoxylated derivatives. Mater Chem Phys 80:169–175

35. Nada F, Atta FAM, Hamdi M, Hassaneen (2011) Electrochemical and antibacterial properties of 316L stainless steel in acid medium containing different newly synthesized organic inhibitors. Int J Hydrog Eng 36(11):6462–6471

36. Fekry AM, Ameer MA (2010) Corrosion inhibition of mild steel in acidic media using newly synthesized heterocyclic organic molecules. Int J Hydrog Eng 34(14):7641–7651

37. Mallaiya K, Subramaniam R, Srikandan SS, Gowri S, Rajasekaran N, Selvaraj A (2011) Electrochemical characterization of the protective film formed by the unsymmetrical Schiff's base on the mild steel surface in acid media. Electrochimi Acta 56:3857–3863. https://doi.org/10.1016/j.electacta.2011.02.036

38. Popova A, Christov M, Raicheva S, Sokolova E (2004) Adsorption and inhibitive properties of Benzimidazole derivatives in acid mild steel corrosion. Corros Sci 46:1333–1350

39. de Oliveira RB, de Souza-Fagundes EM, Soares RPP Andrade AA, Krettli AU, Zani CL (2008) Synthesis and antimalarial activity of semicarbazone and thiosemicarbazone derivatives. Eur J Med Chem 43:1983–1988. https://doi.org/10.1016/j.ejmech.2007.11.012

40. Gupta NK, Verma C, Salghi R, Lgaz H, Mukherjee AK, Quraishi MA (2017) New phosphonate based corrosion inhibitors for mild steel in hydrochloric acid useful for industrial pickling processes: experimental and theoretical approach. New J Chem 41:13114–13129. https://doi.org/10.1039/c7nj01431g

41. Arukalam IO (2014) Durability and synergistic effects of KI on the acid corrosion inhibition of mild steel by hydroxypropyl methylcellulose. Carbohydr Polym 112:291–299. https://doi.org/10.1016/j.carbpol.2014.05.071

42. Gao G, Liang C (2007) Electrochemical and DFT studies of β-amino-alcohols as corrosion inhibitors for brass. Electrochim Acta 52:4554–4559. https://doi.org/10.1016/j.electacta.2006.12.058

43. Hasanov R, Sadikoğlu M, Bilgiç S (2007) Electrochemical and quantum chemical studies of some Schiff bases on the corrosion of steel in H$_2$SO$_4$ solution. Appl Surf Sci 253:3913–3921. https://doi.org/10.1016/j.apsusc.2006.08.025

44. Obot IB, Macdonald DD, Gasem ZM (2015) Density functional theory (DFT) as a powerful tool for designing new organic corrosion inhibitors: Part 1: an overview. Corros Sci 99:1–30. https://doi.org/10.1016/j.corsci.2015.01.037

45. Geerlings P, De Proft F, Langenaeker W (2003) Conceptual density functional theory. Chem Rev 103:1793–1873. https://doi.org/10.1021/cr990029p

46. Chauhan DS, Ansari KR, Sorour AA, Quraishi MA, Lgaz H, Salghi R (2018) Thiosemicarbazide and thiocarbohydrazide functionalized chitosan as ecofriendly corrosion inhibitors for carbon steel in hydrochloric acid solution. Int J Biol Macromol 107:1747–1757. https://doi.org/10.1016/j.ijbiomac.2017.10.050

47. Obot IB, Ebenso EE, Kabanda MM (2013) Metronidazole as environmentally safe corrosion inhibitor for mild steel in 0.5 M HCl: experimental and theoretical investigation. J Environ Chem Eng 1:431–439. https://doi.org/10.1016/j.jece.2013.06.007

48. Idir B, Kellou-Kerkouche F (2018) Experimental and theoretical studies on corrosion inhibition performance of phenanthroline for cast iron in acid solution. J Electrochem Sci Technol 9:260–275

Authors and Affiliations

V. R. Adinarayanan[1] · P. Preethi Kumari[1] · Suma A. Rao[1]

✉ Suma A. Rao
   suma.rao@manipal.edu

[1] Department of Chemistry, Manipal Institute of Technology, Manipal Academy of Higher Education, Manipal 576104, India